Optical Characterization of Ordering and Disordering of Block Copolymer Microstructure

Karl Amundson,* Eugene Helfand, Sanjay S. Patel, and Xina Quan

AT&T Bell Laboratories, Murray Hill, New Jersey 07974

Steven D. Smith

The Procter and Gamble Company, Cincinnati, Ohio 45239

Received November 11, 1991; Revised Manuscript Received December 13, 1991

ABSTRACT: Phenomena associated with the order–disorder transition (ODT) of block copolymers have been studied optically. Observations have been made on symmetric polystyrene-*b*-poly(methyl methacrylate) diblock samples of two molecular weights. Ordering and disordering are clearly indicated by birefringence and a light intensity measurement sensitive to inhomogeneities in microscopic birefringence. The transition temperatures were compared to rheologically-determined ODT temperatures. The optical measurements point to complex behavior near the ODT, including an apparent ~3 °C increase in the disorder temperature upon annealing as well as apparent gradual disordering over a 5–7 °C temperature range. Optical measurements of this type would appear to be a valuable tool for noninvasive study of block copolymers.

Introduction

The order–disorder transition (ODT) of block copolymers, as well as behavior around this transition, has been the focus of much theory and experiment.[1-10] It is of considerable interest because of its relevance to processing, and it is a model for the study of an unusual class of phase transitions.[2-4] The primary means by which transitional behavior has been studied is by rheology[4-8] and scattering,[9,10] both of which reflect the transition from an ordered to a disordered state.

In this paper, we report optical measurements on symmetric polystyrene/poly(methyl methacrylate) diblock copolymer samples near the ODT. We have observed that a birefringence measurement and a light intensity measurement are sensitive indicators of ordering and disordering in these copolymers. In broad terms, the birefringence disappears when the material disorders and reappears when the material orders. The detailed behavior near the ODT is complex, however, and will be the focus of this paper. These optical measurements are sensitive to ordering, disordering, alignment of microstructure, and defect density and should provide information complementary to rheology and scattering on a wide variety of block copolymer systems.

Birefringence and Block Copolymer Microstructure. Form birefringence, the birefringence due to an anisotropic composition pattern, has been observed in aligned, strongly phase-segregated styrene–isoprene block copolymers[11-13] and in polystyrene/poly(methyl methacrylate) block copolymers.[14] In this section, we develop a general expression for the form birefringence which is applicable to block copolymers near the ODT.

In a block copolymer sample, the displacement field, $\mathbf{D}$, is related to the electric field, $\mathbf{E}$, through the relation

$$\mathbf{D}(\mathbf{r}) = \epsilon(\mathbf{r})\,\mathbf{E}(\mathbf{r}) \tag{1}$$

where $\epsilon(\mathbf{r})$ is the local dielectric constant, which is a function of the composition at position $\mathbf{r}$ and is evaluated by coarse-graining over a volume containing many monomers but over a length scale much smaller than molecular dimensions. Since ultimately the electric field we are considering is that of light, the dielectric constant and all subsequent ones defined must be the appropriate values for the frequence of light used.

By averaging eq 1 over a scale larger than molecular dimensions but smaller than the length scale over which the ordered-phase microdomain pattern loses coherence, we can define an effective dielectric constant, $\underline{\underline{\epsilon}}$, associated with a region of coherence in the ordered phase:

$$\overline{\mathbf{D}(\mathbf{r})} = \overline{\epsilon(\mathbf{r})\,\mathbf{E}(\mathbf{r})} = \underline{\underline{\epsilon}}\cdot\overline{\mathbf{E}(\mathbf{r})} \tag{2}$$

where the bar denotes the spatial average. Because of a lack of rotational symmetry of the ordered-phase microdomain pattern, the effective dielectric constant must be expressed as a second-rank tensor.

The effective dielectric constant can be determined by solving the Maxwell equation for the case where there are no free charges:

$$\nabla\cdot\mathbf{D} = \nabla\cdot[\epsilon(\mathbf{r})\,\mathbf{E}(\mathbf{r})] = 0 \tag{3}$$

Assume the local dielectric constant varies linearly with local composition, as expressed by the variable $\psi(\mathbf{r})$, which is the deviation of the volume fraction of one component from its mean value. Below the transition, one expects a periodic lamellar pattern, $\langle\psi\rangle$, to emerge.[1,2] (The angular brackets indicate a time average over a time much larger than the lifetime of composition fluctuations but much smaller than the time over which the ordered-phase microdomain pattern changes.) Equations 2 and 3 can be solved to second order in $\langle\psi\rangle$ to yield

$$\underline{\underline{\epsilon}} = \epsilon_D\underline{\underline{\mathbf{I}}} - \frac{(\epsilon_1-\epsilon_2)^2}{\epsilon_D}\overline{\langle\psi\rangle^2}\hat{\mathbf{e}}_k\hat{\mathbf{e}}_k \tag{4}$$

where ϵ_1 and ϵ_2 are the dielectric constants of the two pure components (again evaluated at the frequency of light). ϵ_D is the dielectric constant in the limit of vanishing microdomain pattern and contains a contribution from the dynamic composition fluctuations whose correlation length is much smaller than the wavelength of light. $\underline{\underline{\mathbf{I}}}$ is the identity matrix, and $\hat{\mathbf{e}}_k$ the unit wave vector of the lamellar pattern. Using the relation $\underline{\underline{\mathbf{n}}}^2 = \underline{\underline{\epsilon}}$ (in Gaussian units), the refractive index tensor, $\underline{\underline{\mathbf{n}}}$, to second order in $\langle\psi\rangle$, is

$$\underline{\underline{\mathbf{n}}} = n_0\underline{\underline{\mathbf{I}}} - \frac{(n_1^2-n_2^2)^2}{2n_0^3}\overline{\langle\psi\rangle^2}\hat{\mathbf{e}}_k\hat{\mathbf{e}}_k \equiv n_0\underline{\underline{\mathbf{I}}} + 4\Delta n^0\overline{\langle\psi\rangle^2}\hat{\mathbf{e}}_k\hat{\mathbf{e}}_k \tag{5}$$

n_1 and n_2 are the refractive indices of the pure components,

0024-9297/92/2225-1935$03.00/0

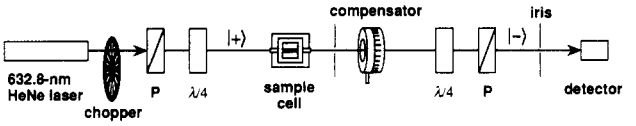

Figure 1. Apparatus for optical measurements. The laser beam passed through a chopper and then through a polarizer (P) and a quarter-wave plate (λ/4) to produce right-circular polarization. After the beam passed through the sample cell and compensator, a quarter-wave plate and polarizer filtered out right-circular polarization. The left-circularly-polarized portion of the beam was measured with a photodetector and a lock-in amplifier.

n_0 the refractive index in the limit of vanishing microdomain pattern, and Δn^0 the maximum form birefringence strength for complete microphase segregation (defined in the above expression). From refractive index data for polystyrene and poly(methyl methacrylate) reported by Michel et al.,[15] Δn^0 for a symmetric polystyrene-*b*-poly(methyl methacrylate) copolymer is computed to be -4.0×10^{-3} at 160 °C and is expected to drop only slightly (~6%) upon heating to 260 °C.

For light propagation at an angle θ to $\hat{\mathbf{e}}_k$, eq 5 yields a form birefringence of

$$\Delta n_{form} = 4\Delta n^0 \overline{\langle\psi\rangle^2} \sin^2\theta \qquad (6)$$

with a "fast" axis along the projection of $\hat{\mathbf{e}}_k$ in the plane perpendicular to the optical trajectory. In the limit of strong phase segregation, $\overline{\langle\psi\rangle^2} = 1/4$, and eq 6 reduces to the familiar form birefringence of the symmetric "stacked-plate" morphology.[12,16] Light polarized along the "slow" axis will experience a phase retardation of magnitude

$$\delta = 2\pi\frac{l}{\lambda}\Delta n^0 \overline{\langle\psi\rangle^2} \sin^2\theta \qquad (7)$$

with respect to light polarized along the "fast" axis, where l is the optical path length and λ is the wavelength of light in the medium (420 nm for 633-nm He–Ne laser light).

If chain extension due to microphase separation is significant, molecular birefringence will also be present. This contribution can be very significant for strongly-segregated block copolymer lamellar systems[12,14] but should be small near the ODT. If it is present, it will add an additional negative quantity to the already-negative form birefringence.[14,17-19]

Experimental Section

Materials. Polystyrene/poly(methyl methacrylate) diblock copolymer samples were synthesized anionically. Their molecular weight averages were 37 000 and 31 000 (polydispersity indices 1.08 and 1.07, respectively), as determined by size exclusion chromatography using polystyrene standards. These are referred to as SM-37 and SM-31, respectively. Both copolymers are 53 vol % polystyrene as determined by ^{1}H NMR. Rheological measurements[20] were made using a Rheometrics 7700 dynamic mechanical spectrometer with a parallel-plate fixture. Electron micrographs reveal that these materials have a lamellar microstructure at low temperature.

Optical Analysis. The optical apparatus is shown in Figure 1. The 632.8-nm He–Ne laser light was made right-circularly polarized by passage through a polarizer and quarter-wave plate. It then passed through the sample cell and a Babinet-Soleil compensator. A quarter-wave plate and polarizer before the detector filtered out right-circular polarization, and so the detector measured only left-circular polarization intensity. The phase retardation and orientation of the compensator were adjusted to minimize light intensity at the detector; the compensator readings then indicated the sample birefringence strength and principal axes. The minimized light intensity was also recorded. Imperfections in optical components introduced systematic errors in the birefringence strength measurements on the order of 30 mrad.

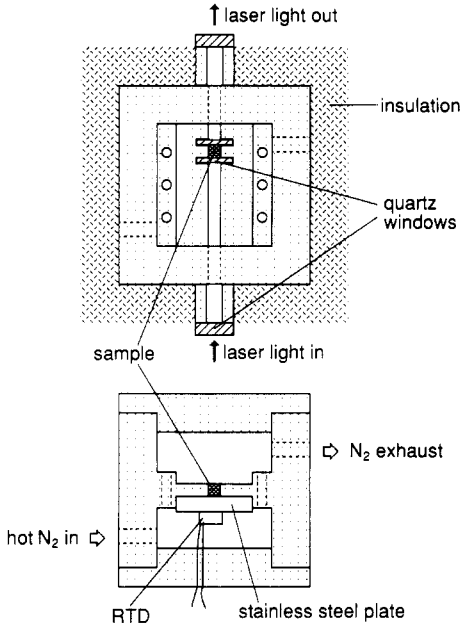

Figure 2. Top and side cross-sectional views of the sample cell.

The sample cell is shown in Figure 2. The laser light passed through quartz windows and a rectangular channel in the center platform of the cell. Two rectangular windows contained the polymer sample within a 2-mm section of the channel. A stainless steel plate pressed tightly against the center platform made up the floor of the sample region. The temperature was controlled (±0.2 °C) with a thermally regulated nitrogen gas purge. A platinum resistance temperature detector bolted to the stainless steel plate from below was used to measure temperature and was calibrated with a thermocouple embedded in a polymer sample. The temperature of the sample cell was also calibrated against the Rheometrics dynamic mechanical spectrometer used in the rheological measurements. The time lag between temperature changes of the sample and the temperature detector reading was 20–25 s.

Results

Figure 3 shows the low-frequency elastic moduli of both copolymers in oscillatory shear. (A full description of the rheology is presented in ref 20.) The ODT, signaled by a drop in the elastic modulus, is at 251 ± 1 and 182 ± 2 °C for SM-37 and SM-31, respectively. Data were collected in the order of increasing temperature.

Figures 4 and 5 show the birefringent phase retardation and minimized light intensity for SM-37 and SM-31 during slow cooling and subsequent slow heating. The cooling and heating rates were 0.2 °C/min near the transition region and somewhat faster far away from the transition region. At high temperature, the birefringence strength was a constant small value, and at low temperature it was nonzero and decreasing with increasing temperature.

After the first thermal cycle, the SM-31 sample was heated a second time to 180 °C, annealed for 5 h, and then very slowly heated (<0.02 °C/min) (with another 14-h anneal at 186 °C) until the optical measurements returned to their high-temperature values. During annealing at 180 °C the birefringence strength grew tenfold (Figure 5). The birefringence persisted up to 183 °C where it began to drop until it finally dissipated at 191 °C. It should be noted that during the 14-h anneal at 186 °C the birefringence strength was almost constant.

The minimized light intensity data paralleled the birefringence data in all experiments. Upon cooling, it rose from a small, constant value beginning at the point where birefringence appeared, and upon heating, it dissipated

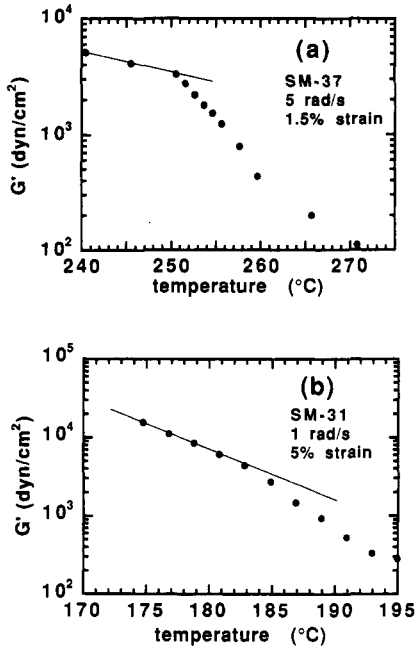

Figure 3. Elastic moduli of (a) SM-37 and (b) SM-31 as a function of temperature. The disorder point is indicated by a sudden decline in the elastic modulus beyond the low-temperature trend. More complete data sets and discussion can be found in ref 20. The lines indicate the trend of the rheological behavior of the ordered phase so that the transition can be more readily seen.

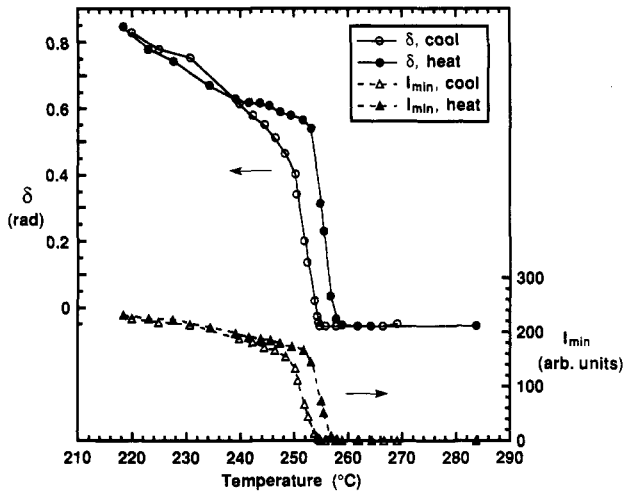

Figure 4. Birefringent phase retardation and minimized light intensity data for SM-37 during cooling from the disordered phase (−0.2 °C/min) and subsequent heating (0.2 °C/min).

along with the birefringence strength. For simplicity, only a portion of the minimized light intensity data upon heating (and for the second heating only) is shown in Figure 5.

The temperature of the SM-37 sample was held at 255 °C in a second heating run; the isothermal birefringent phase retardation and minimized light intensity data are shown in Figure 6. Upon annealing at that temperature, the birefringence strength dropped to one-third its initial value in ~30 min, then recovered to two-thirds its original value over the next 30 min, and remained constant over the next 150 min. This type of behavior, where the birefringence strength dropped upon an increase in temperature followed by slow growth, was observed in numerous other instances for SM-31 as well, when the temperature was near the ODT. Measurements during subsequent thermal scans showed that these changes in optical measurements could not be attributed to sample

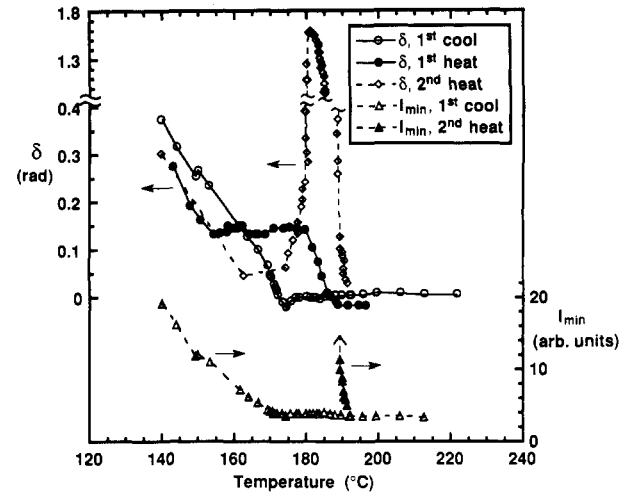

Figure 5. Birefringent phase retardation and minimized light intensity data for SM-31 during cooling from the disordered phase (−0.2 °C/min) and subsequent heating (0.2 °C/min) and during a second anneal and slow heating (≤0.02 °C/min). For simplicity, only some of the minimized light intensity data taken during heating are shown (and for the second heating run only).

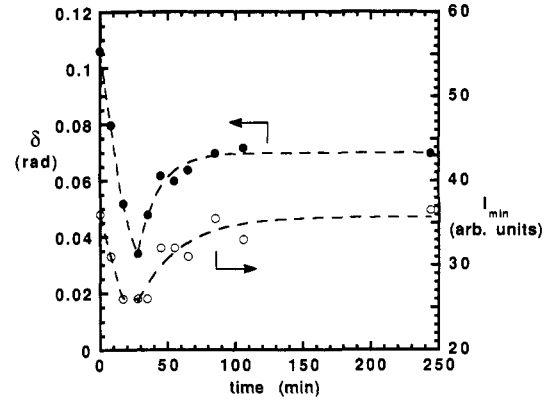

Figure 6. Transient isothermal birefringent phase retardation and minimized light intensity data for SM-37 at 255 °C. The curves through the data are drawn merely as aids.

degradation, because once the material was disordered, it exhibited the original birefringence behavior.

Discussion

Both the birefringence and the minimized light intensity exhibit rapid transitions near the rheologically-determined ODT, as shown in Figures 4 and 5. Before discussing the details of the transition behavior of the two copolymers, we explore the relationship of the optical measurements to microstructure.

Optical Measurements and the Disordered Phase. The disordered phase does not possess long-range order but will exhibit concentration fluctuations that grow as the transition is approached.[1,2,5] Since these fluctuations do not exhibit a preferred orientation, the sample will not be birefringent. Also, the correlation length for fluctuations in copolymer samples used in this study is not expected to greatly exceed molecular dimensions.[21] Therefore, the material will appear isotropic on the length scale of the wavelength of light (which is much larger than molecular dimensions), and the minimized light intensity will be small (see discussion below). This is observed at high temperature for both copolymers (Figures 4 and 5).

Optical Measurements and the Ordered Phase. The low-temperature behavior of the birefringence strength and minimized light intensity for both copolymers are similar: each is nonzero and decreases with increasing

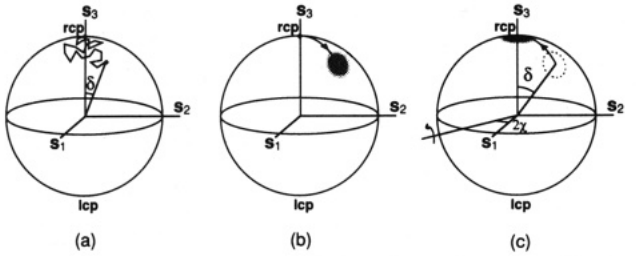

Figure 7. Representation of light polarization using Stokes parameters and the Poincaré sphere. s_1, s_2, and s_3 are Stokes parameters. (a) shows a "random walk" representing evolution of light polarization as it passes through one particular microstructural arrangement in an ordered-phase block copolymer sample. (b) shows the (mixed) state of polarization of a (thick) laser beam after passing through an ordered-phase block copolymer sample. Anisotropy in lamellar alignment causes the distribution to be centered away from the north pole, and the distribution spread is due to variations in microstructural arrangements experienced by different portions of the laser beam. (c) shows the action of the compensator when it is adjusted to minimize light intensity at the detector.

temperature. In this section, we describe how the measurements and trends relate to ordered-phase morphology.

Electron micrographs of the copolymers used in this study reveal a lamellar microstructure with typical defect structure. The orientational correlation length scale is on the order of several microns. The effect of the microstructure on the polarization of light can be understood, within limits, using the Stokes parameters for light polarization. (A discussion of Stokes parameters can be found in ref 16, 22, and 23.) The polarization state of light can be put into correspondence with a point on a sphere representing two independent Stokes parameters. This sphere is called the Poincaré sphere;[16,22] the "north pole" corresponds to right-circular polarization, the "south pole" to left-circular polarization, and the "equator" to linear polarization along an axis that varies with longitude. This representation is particularly convenient because the effect of the birefringence of each "region of coherence"[24] on the polarization of light passing through it can be represented by a small rotation of the point on the Poincaré sphere, where the rotation axis and magnitude are determined by the orientation, birefringence strength, and size of the region. From eq 7 and an estimate for $\langle\psi\rangle^2$ just below the ODT of $\sim$0.1,[25] the rotation associated with a 5-μm region is $\sim$15 mrad. (Reflections and refractions associated with spatial variations in the refractive index tensor are ignored because the variations are small ($\Delta n_{\text{form}}/n \sim 10^{-3}$).) The consequence of passage through a series of regions of coherence is a series of uncorrelated small phase retardations, and the associated trajectory on the Poincaré sphere is a special "random walk" made up of a series of small rotations and beginning at the north pole (Figure 7a). The effective birefringent retardation is determined by the latitude of the end point of the random walk, and the effective principal axes are determined by the longitude of the end point.

An additional important consideration is that the $\sim$0.8-mm-diameter laser beam is far wider than any region of coherence of the polymer microstructure. Light with trajectories separated by more than a few microns will travel through different microstructural arrangements, and their polarization evolutions will be represented on the Poincaré sphere by different "random walks". The polarization of the exiting laser beam will therefore be a *mixed* state, represented by a distribution of points on the Poincaré sphere. If, in addition, the microstructure is preferentially aligned, the propagation of light polarization will be represented on the Poincaré sphere as a mixture of *biased* "random walks", and the distribution of points representing the final mixed state of polarization will be centered at some position away from the north pole. This situation is illustrated in Figure 7b.

We are now in a position to understand the relationship of the birefringence and minimized light intensity measurements to microstructure. The action of the compensator, shown in Figure 7c, is represented as a rotation on the Poincaré sphere, with an axis defined by the compensator crystal axis and a rotation angle corresponding to its retardation strength. The compensator can always be adjusted to transform any pure state of polarization (a point on the Poincaré sphere) to pure right-circular polarization (the north pole). A mixed state, however, cannot be transformed to right-circular polarization, just as a distribution of points cannot be mapped to the north pole by a single rotation. Instead, the light intensity at the detector is minimized when the compensator rotates the distribution of points on the Poincaré sphere so it is centered on the north pole (Figure 7c). Various parts of the laser beam still will have some left-circular polarization, and since they are spatially resolved, they will add to the minimized light intensity.[26] The broader the distribution of polarization states, the greater the minimized light intensity will be.

Therefore, the two optical measurements provide complementary information on the sample microstructure. The compensator settings for which light intensity at the detector is a minimum indicate an "average" birefringence property of the sample and are a measure of the macroscopic alignment of microstructure. The minimized light intensity is a measure of the inhomogeneity of the laser beam polarization, which in turn indicates inhomogeneity of microstructure orientation.

The appearance of birefringence and sudden rise in the minimized light intensity upon cooling of the copolymer samples indicate formation of an ordered phase. The increase in minimized light intensity reflects spatial inhomogeneity in the form birefringence associated with imperfect ordering. While macroscopic birefringence can only be exhibited by the ordered phase, its cause is not immediately evident. One would not expect any particular "fast" axis direction if there were not a preference for lamellar orientation. Nonetheless, macroscopic alignment is indicated by the presence of birefringence, and we can only speculate over its cause. The principal "fast" birefringence axis of the SM-37 sample remained between 0 and −5° from the vertical for most of the experiments (although it changed to −20 to −25° after a second cooling from the disordered phase), and for SM-31 it remained between 4 and 7° from the vertical throughout experiments. This shows that lamellae have a very slight preference toward horizontal alignment (cf. Figure 2, side view). Surfaces can induce alignment,[27] but this effect is considered not to be of sufficient range to persist into the bulk. Another factor is that temperature gradients, if any, are expected to be in the vertical direction. Because the nitrogen purge enters the lower half of the sample cell, that half should cool slightly earlier than the upper half during cooling. A small vertical temperature gradient could result in a growth front of ordered phase from the lower surface upward, leading to a greater impact of the lower surface on bulk alignment than otherwise expected. A coupling between orientation and a temperature gradient has been reported in crystalline[28] and liquid crystal systems,[29] for example. Stress due to differences in thermal expansion coefficients between the sample cell

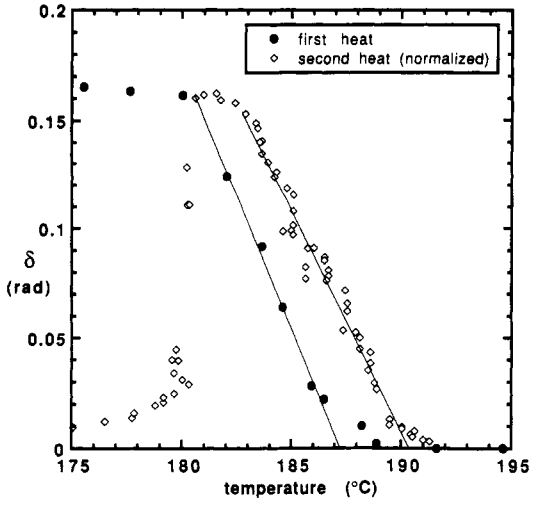

Figure 8. Birefringent phase retardation for SM-31 during the first heating (0.2 °C/min) and the second heating (≤0.02 °C/min). The small high-temperature phase retardation (due to instrumental error) has been subtracted and the data for the second sweep have been normalized to match the first at 180 °C. Lines indicate best linear fits to the data in the transition region.

and sample is another possible cause of macroscopic alignment. Anisotropy in neutron scattering patterns from polyalkane block copolymers cooled through the ODT has been attributed to this effect.[30] It should be noted that only a very small anisotropy is necessary to explain the observed birefringence. A comparison of the measured birefringence strength to the value anticipated from eq 6 gives a Hermans' orientational order parameter[31] on the order of 10^{-2}, a quantity smaller than can be readily detected by scattering, for example.

The increase in form birefringence and minimized light intensity upon cooling below the disorder point reflect increasing microphase segregation ($\langle\psi\rangle^2$ in eq 6) upon cooling and possibly increased chain stretching. The birefringence strength of SM-31 "wanders" somewhat upon slow heating between 155 and 180 °C (Figure 5). This is presumably due to annealing of defect structures once the material reaches sufficient mobility.

Transition Behavior. Complex behavior near the ODT is revealed by the optical measurements. Upon slow cooling, the birefringence and minimized light intensity measurements for SM-31 begin to rise at 175 °C, indicating that the ordered phase first appears at that temperature. Upon heating, the sample loses its birefringence at ~187 °C, indicating loss of long-range order at that temperature. Also, the birefringence begins to drop sharply beginning ~7 °C below that temperature. This drop could initially be interpreted as slow disordering over ~35 min beginning at 180 °C. However, the behavior during the second heating cycle suggests this is not so. In Figure 8 the birefringence data for the two heating cycles are compared. (The data for the second heating were normalized by matching the birefringence strength of the first at 180 °C.) Even though the heating rate was over 10 times slower than for the first heat and the sample was held at the midpoint of the transition range (186 °C) for 14 h, both data sets show the same trend—a sharp drop in magnitude, but over a ~7 °C range. SM-37 shows qualitatively similar behavior; both optical measurements show a sharp drop, but over a 5 °C range before complete disordering.

The unexpected behavior of the optical measurements in a range of 5–7 °C before complete disordering is not well understood and is under investigation. It is important to keep in mind that the ordered-phase material as a rule is not in its equilibrium state. Equilibrium is difficult to attain because of the long time for annealing of imperfect lamellar structure. We speculate that the gradual decrease in optical parameters before disordering indicates some sort of spatially-heterogeneous disordering associated with nonequilibrium fluctuations of structure. In contrast, an ordered-phase material at equilibrium would show a sharp disordering transition. This speculation is supported by the results of experiments where the sample temperature was increased a small amount near the disorder point, with the result that the birefringence dropped significantly and then grew over a period of hours (as in Figure 6, for example). This suggests partial disordering, followed by reordering of a more perfect ordered phase.

The data from the second heat of SM-31 reveal other interesting facts as well. The large rise in the birefringence strength upon annealing at 180 °C indicates a change in the degree of macroscopic alignment, and the large minimized light intensity (as compared to the first thermal cycle) suggests a coarser-grained, more perfect ordered structure.[32] In addition, the disordering behavior is ~3 °C higher than for the first thermal scan (see Figure 8), presumably due to the increased order. An analogy is the effect of crystal size on the melting point, where smaller crystals melt at a lower temperature than larger ones.[33] This observation could have important ramifications for rheological determination of the order–disorder transition. It is possible that the flow field of a rheological experiment could affect the long-range order, perhaps by inducing macroscopic alignment or introducing new defects through rotation of order not totally perpendicular to the flow direction. Such changes could alter the apparent temperature at which disordering occurs by a small amount, just as the disordering temperature of the SM-31 copolymer increased 3 °C along with perfecting of structure associated with annealing.

Comparison between the rheologically-determined ODT temperature and the optically-determined ordering and disordering behavior will not be reliable until the processes occurring during both are better understood. The rheologically-measured ODT temperature for SM-31 (182 ± 2 °C) is between the optically-determined ordering temperature (175 °C) and disordering temperature (187–191 °C, depending upon thermal history). For SM-37, the rheologically-determined ODT temperature is 251 ± 1 °C, while the optically-determined ordering and disordering temperatures (for 0.2 °C/min heating and cooling) were 254 and 257 °C, respectively. The discrepancy between the "rheological ODT temperature" and the "transition temperature range" indicated by the optical measurements is somewhat larger than can be explained by the 1–2 °C uncertainty in temperature measurements. In principal, the discrepancy could be due to differences in thermal histories of samples in the two experiments and the effect of shear on the ordered phase, but then one would expect similar discrepancies to exist for both copolymers, and this is not the case.

Conclusions

Ordering and disordering of two polystyrene/poly(methyl methacrylate) block copolymers were characterized by two optical measurements on a birefringence apparatus: a birefringence measurement sensitive to very slight macroscopic alignment of the ordered phase and a "minimized light intensity" measurement sensitive to inhomogeneities present in the ordered phase. Both measurements are strong indicators of ordering and disordering

of block copolymer samples, and reasonable agreement is found with rheological determinations of the ODT temperature. The optical measurements reveal complex behavior near the ODT including an elevation of the disorder temperature upon annealing and an apparent gradual disordering over a 5–7 °C range before complete disordering. We anticipate applicability of this technique to other block copolymer melts and solutions involving lamellar or cylindrical microstructures. (Form birefringence will not be exhibited by spherical and ordered-bicontinuous double-diamond morphologies, by symmetry.) The two optical measurements should be able to provide information complementary to rheology and scattering experiments because of their high sensitivity to macroscopic alignment and defect texture.

Acknowledgment. We thank Arman Ashraf for assistance in the synthesis and characterization of materials.

References and Notes

(1) Leibler, L. *Macromolecules* **1980**, *13*, 1602.
(2) Fredrickson, G. H.; Helfand, E. *J. Chem. Phys.* **1987**, *87*, 697.
(3) Fredrickson, G. H.; Binder, K. *J. Chem. Phys.* **1989**, *91*, 7265.
(4) Bates, F. S.; Fredrickson, G. H. *Annu. Rev. Phys. Chem.* **1990**, *41*, 525.
(5) Bates, F. S.; Rosedale, J. H.; Fredrickson, G. H.; Glinka, C. J. *Phys. Rev. Lett.* **1988**, *61*, 2229.
(6) Bates, F. S. *Macromolecules* **1984**, *17*, 2607.
(7) Chung, C. I.; Gale, J. C. *J. Polym. Sci., Polym. Phys. Ed.* **1976**, *14*, 1149.
(8) Gouinlock, E. V.; Porter, R. S. *Polym. Eng. Sci.* **1977**, *17*, 535.
(9) Hashimoto, T.; Kowsaka, K.; Shibayama, M.; Kawai, H. *Macromolecules* **1986**, *19*, 754.
(10) Harkless, C. R.; Singh, M. A.; Nagler, S. E.; Stephenson, G. B.; Jordan-Sweet, J. L. *Phys. Rev. Lett.* **1990**, *64*, 2285.
(11) Folkes, M. J.; Keller, A. *Polymer* **1971**, *12*, 222.
(12) Folkes, M. J.; Keller, A. *J. Polym. Sci., Polym. Phys. Ed.* **1976**, *14*, 833.
(13) Folkes, M. J.; Keller, A.; Odell, J. A. *J. Polym. Sci., Polym. Phys. Ed.* **1976**, *14*, 847.
(14) Chin, I.; Smith, B. A.; Russell, T. P., personal communication.
(15) Michel, P.; Dugas, J.; Cariou, J. M.; Martin, L. *J. Macromol. Sci., Phys.* **1986**, *B25*, 379. Data for 578-nm light are given. We make no correction for differences in refractive index between 578-nm and 632.8-nm light.
(16) Born, M.; Wolf, E. *Principles of Optics*; Pergamon Press: New York, 1959.
(17) Stein, R. S. *J. Appl. Phys.* **1961**, *32*, 1280.
(18) Faivre, J. P.; Xu, E.; Halary, J. L.; Jasse, B.; Monnerie, L. *Polymer* **1987**, *28*, 1881.
(19) Kashiwagi, M.; Folkes, M. J.; Ward, I. M. *Polymer* **1971**, *12*, 697.
(20) Patel, S. S.; Helfand, E.; Quan, X.; Amundson, K. R.; Smith, S. D., submitted for publication in *Macromolecules*.
(21) Equations 5.1 and 5.3 and associated equations of ref 2 were used to calculate that the correlation length of fluctuations at the ODT is 10–20 nm. This is only an estimate, since the molecular weights used here are much less than required for applicability of the theory.
(22) Kliger, D. S.; Lewis, J. W.; Randall, C. E. *Polarized Light in Optics and Spectroscopy*; Harcourt Brace Jovanovich: New York, 1990.
(23) Jackson, J. D. *Classical Electrodynamics*, 2nd ed.; John Wiley & Sons: New York, 1975; p 848.
(24) The "region of coherence" is a fiction we have adopted for convenience. Within a "region of coherence", the microstructure is considered uniform and uncorrelated with surrounding microstructure. In reality, microstructure orientation exhibits slow, continuous changes as well as sharp changes at defects.
(25) $\langle\psi\rangle^2$ is predicted using eqs 3.8 and 4.4 of ref 2 (where $\bar{N}$ was used instead of N in eq 4.4). $\bar{N}$ is defined in: Fredrickson, G. H.; Binder, K. *J. Chem. Phys.* **1989**, *91*, 7265 (eq 2.9).
(26) Not included in the discussion is the effect of interference between the electric fields of light emerging from the spatially-distinct paths through the sample. Because of interference, the electric field pattern at the compensator will not be the same as the electric field pattern of light leaving the sample. Nonetheless, the electric field at each point on the detector will be a different linear combination of electric fields leaving the sample, with the appropriate transformations for propagation through space and optical components (see, for example, Chapter 8 of ref 16). Therefore, if light polarization leaving the sample is spatially inhomogeneous, it will also be spatially inhomogeneous at the compensator and the minimized light intensity will be large. In addition, interference between spatially-resolved portions of the laser beam within the sample can only further mix the light state.
(27) Russell, T. P.; Coulon, G.; Deline, V. R.; Miller, D. C. *Macromolecules* **1989**, *22*, 4600.
(28) Cladis, P. E. *J. Stat. Phys.* **1991**, *64*, 1103.
(29) Cladis, P. E.; Gleeson, J. T.; Finn, P. L.; Brand, H. R. *Phys. Rev. Lett.*, in press.
(30) Bates, F., personal communication.
(31) Hermans, J. J.; Hermans, P. H.; Vermaas, D.; Weidinger, A. *Recl. Trav. Chim. Pays-Bas* **1946**, *65*, 427. Although the relationship between the birefringence strength and the Hermans' order parameter is only rigorously valid when the length scale of variations is smaller than the wavelength of the light, we assume that it can be used in at least an approximate sense in this case as well.
(32) A coarsening of the defect texture will result in a larger rotation on the Poincaré sphere associated with each "region of coherence" in the sample, and since the optical path remains constant, the contour length of the random walk will not change. The result is a greater mean-square birefringence strength due to inhomogeneities in the sample, and thus a greater minimized light intensity. An analogy is the end-to-end distance of a polymer in a Θ solvent. If the persistence length of the chain increases while its contour length is fixed, the end-to-end distance will increase in proportion to the square root of the persistence length.
(33) Wunderlich, B. *Macromolecular Physics: Crystal Melting*; Academic Press: New York, 1980; Vol. 3.

Registry No. (St)(MMA) (block copolymer), 106911-77-7.